Article

Gel dosimetry with radio-fluorogenic coumarin

Peter A. Sandwall [1,*], Brandt P. Bastow [2], Henry B. Spitz [2], Howard R. Elson [2], Michael Lamba [2], William B. Connick [2] and Henry Fenichel [2]

[1] OhioHealth; Mansfield, Ohio
[2] University of Cincinnati; Cincinnati, Ohio
* Correspondence: pasandwall@gmail.com; Tel.: +1-513-307-8156

Abstract: In radiotherapy, accurate deposition of energy to the targeted volume is vital to ensure effective treatment. Gel dosimeters are attractive detection systems, as tissue substitutes with potential to yield three-dimensional dose distributions. Radio-fluorogenesis is creation fluorescent chemical products in response to energy deposition from high-energy radiation. This report shares studies of a radio-fluorogenic gel dosimetry system, gelatin with coumarin-3-carboxlyic acid (C3CA), for the quantification of imparted energy. Aqueous solutions exposed to ionizing radiation result in the production of hydroxyl free radicals through water radiolysis. Interactions between hydroxyl free radicals and coumarin-3-carboxylic acid produce a fluorescent product. 7-hydroxy-coumarin-3-carboxylic acid has a blue (445 nm) emission, following UV to near UV (365–405 nm) excitation. Effects of C3CA concentration and pH buffers were investigated for this system. The response of the system was explored with respect to strength, type, and exposure rate of high-energy radiation. Results show a linear dose response relationship with a dose-rate dependency and no energy or type dependencies. This report supports the utility of gelatin-C3CA for phantom studies of radio-fluorogenic processes.

Keywords: gel dosimetry; radiation dosimetry; radio-fluorogenic gel, luminescent dosimetry

1. Introduction

Advancements in radiation therapy technology have supported study of tissue-equivalent gels containing active chemical sensors for the measurement of absorbed dose of radiation. Gel dosimeters have radiological properties similar to biological tissue and are suitable substitutes with the potential to resolve three-dimensional dose distributions. The development of gel dosimeters was dormant for many years, but has recently been developing at a rapid pace. The first reported use of a gel dosimeter was in 1950 with the colorimetric dye methylene blue [1]. Other early investigators explored chloral hydrate and trichloroethylene in agar [2]. Gelatin with ferricyanide, Fricke-type, gel dosimeters were first studied using colorimetric methods, and later magnetic resonance (MR) imaging [3-5]. Further developments introduced polymer and leuco-dye systems [6-7]. Recently, a radio-fluorogenic polymer system has been introduced [8]. Each of the current gel dosimeters have their own limitations such as rapid diffusion of chemical products with Fricke-type, toxicicty of with polymer systems, intricate fabrication methods with leuco-dyes, and the water-insolubility of radio-fluorogenic polymers [9]. The hunt for the ideal sensor element and gel substrate is ongoing.

Two of the most common gel substrates are agarose and gelatin. Gelatin is derived from bovine or porcine collagen; primary element of skin, bone, and connective tissue. Agarose is a polysaccharide isolated from agar with highest gelling potential; agar is derived from seaweed. Gelatin and agarose are both capable of creating hydrogels with low percentages of gelling agent. However, agarose is opaque and induces light scattering, while gelatin is relatively translucent. The opacity of agar makes it less than ideal for optical analysis.[32] Clarity and transparency of gelatin is

strongly dependent on raw material history, purity, and preparation. Commercial gelatin consists of tropocollagen rods in the order of 300 nm in length with 1.5 nm diameter [10]. Raw material is processed with acid or base solutions yielding "Type A" (hydrogen chloride) or "Type B" (sodium hydroxide). Type A is denser than type B with a greater intrinsic viscosity [11]. Gelation speed also affects rigidity with structure a function of formation temperature, slow gelatin yields increased organization and orientation of chain elements with greater lateral bonding, this results in the formation of fine well-ordered lattices [12]. Additionally, gelation is not susceptible to ionic effects [10]. Derived from biological tissue with well understood mechanisms of gelation, gelatin is an attractive substrate for exploration of optically active sensors.

Radio-fluorogenic sensors are chemical elements that allow for dosimetry, quantification of energy deposition from of ionizing radiation, through measurement of molecular fluorescence. Fluorescent detection methods are particularly promising due to their ability to form selective high-resolution images. Initially reported by Day and Stein in 1949, fluorescence spectroscopy can be used to determine absorbed dose in aqueous solutions of aromatic compounds [13-15]. Ionizing radiation initiates radiolysis of water, yielding hydroxyl free radicals that hydroxylate aromatic compounds via electrophilic substitution. Numerous aromatic compounds are recognized as radio-fluorogenic, with hydroxylation producing fluorescent products. The first fluorescent sensor investigated for radiation dosimetry was aqueous benzoic acid [15]. Other potential sensors are terephthalic, trimesic, and pyromellitic acid [16-18]. Each improved the yield of fluorescent products by restraining positions for substitution. However, each of those compounds possesses excitation wavelengths unsuitable for a gel substrate. Rayleigh scattering is wavelength dependent, proportional to $1/\lambda^4$, resulting in rapid reduction of transmission for shorter wavelengths of light. Organic gels are naturally turbid due to their macromolecular nature, thus it is preferable to use longer excitation wavelengths with greater potential for penetration. Fluorescence of aromatic compounds is due to their conjugated system of alternating single and double-bonds; overlapping pi-orbitals allow for delocalization of electrons. Larger conjugated systems require less energy for excitation [19]. Selection of a multi-cyclic radio-fluorogenic sensor would provide a more attractive fluorescent product; ideally with excitation from visible light. Multi-cyclic coumarin-3-carboxylic acid (C3CA) is a sensor candidate.

Aqueous C3CA has been identified as chemical dosimeter for application to radiotherapy with favorable traits including linear dose response, reproducibility, and long-term stability [20]. The radio-fluorogenic mechanism of C3CA has been studied within aqueous solution [21]. Positive features of C3CA include high solubility in aqueous solutions, simple organic composition, and favorable excitation and emission spectra. C3CA reacts with hydroxyl radicals to yield the fluorescent product, 7-hydroxycoumarin-3-carboxylic acid (7HOC3CA), Figure 1.

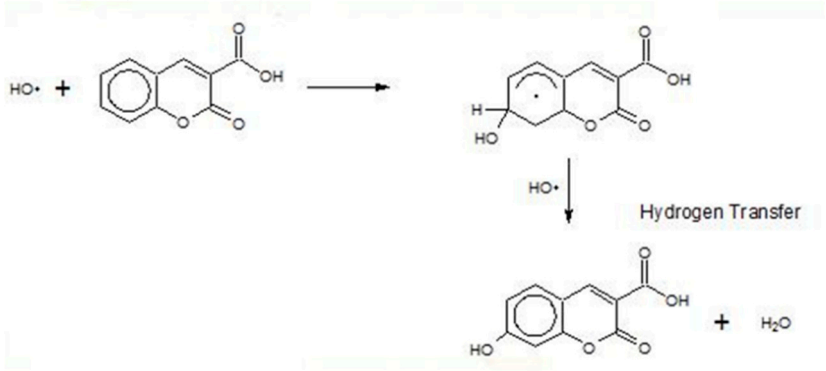

Figure 1. Hydroxyl radicals react with C3CA to yield 7HOC3CA through hydrogen abstraction, transfer, and substitution.

The present investigation explored C3CA in gelatin as a potential radio-fluorogenic detector. Concentration effects of C3CA were studied and the influence of pH buffers was investigated with

respect to relative fluorescent yield. Ionizing radiation response was examined subject to dose, rate, energy, and type for megavoltage electron and photon energies.

2. Materials and Methods

Solutions were readied with water from EASYpure water purification system (Barnstead International). Reagents were procured from Fisher Scientific (Baltimore, MD): 98% C3CA, C10H6O4 (Acros Organics, Baltimore, MD) and 99% 7HOC3CA, C10H6O5, MW 206.16 (Infodine Chemical Company; Hillsborough, NJ), sodium bicarbonate, sodium hydroxide, phosphate buffered saline, and food grade porcine type A gelatin (bloom strength 260, pH 5, and viscosity 40). Aliquots were separated, irradiated, and analyzed. Samples were stored at low temperature (5° C) to inhibit microbial growth.

To allow for dispersion, gelatin was 'wet,' placed in a beaker to soak with half the total volume of water for 20 minutes. C3CA was brought into solution by boiling a small volume in a separate beaker. After sufficient 'wetting', aqueous C3CA solution was added with the remaining portion of water and temperature of gel solution raised to 35° C; care was taken to ensure the temperature remained below 40° C to prevent denaturation. Gel was maintained at 35° C for 90 minutes, or until optically clear and free of visible colloidal structures. The solution was then removed from heat and pipetted into poly-methyl-methacrylate (PMMA) cuvettes. Gels were left to cool overnight at ambient temperature. For initial pH buffer studies, 7% gelatin solutions were made with 7HOC3CA to mimic the radio-fluorogenic product. Sodium bicarbonate/hydroxide and phosphate buffered saline (PBS) solutions were prepared with 0.9 mM C3CA and 0.1 mM 7HOC3CA. For concentration and dose response studies, 1 mM, 5 mM, 10 mM, and 20 mM C3CA solutions were prepared with the sodium bicarbonate/hydroxide buffer.

Irradiations were conducted with a C-series high-energy medical linear accelerator (linac) (Varian Medical Systems; Palo Alto, CA), with two megavoltage (MV) photon and five electron energies; 6 and 23 and 6, 9, 12, 15, and 20 MeV. Irradiations were conducted with a polystyrene phantom containing a void for 4 cuvettes; the phantom was designed expressly to provide geometry favorable for establishment of electronic equilibrium. A computed tomography (CT) scan was carried out on the phantom, images were imported into Eclipse treatment planning system (Varian Medical Systems; Palo Alto, CA), and nominal dose calculated.

Instrumental analysis was conducted with a Cary Eclipse fluorescence spectrophotometer (Varian, Inc.; Pal Alto, California). Excitation and emission slit widths were set to 5 nm, emission scans were performed and peak emission values recorded and plotted. The dose response curve was created by plotting intensity of 445nm emission versus nominal dose.

3. Results

3.1. pH Response

The influence of pH buffers on fluorescent response was examined. Several solutions yielded various pH's; deionized water (pH 6.0), phosphate buffered saline (pH 7.4), and sodium hydroxide with sodium bicarbonate (pH 10). Results show positive correlation between pH and quantum yield. A spectral shift of the excitation maxima was also demonstrated. Specifically, peak excitation shifted from 365nm in normal (pH 7) solution to 405 nm in basic (pH = 10) solution, Figure 2.

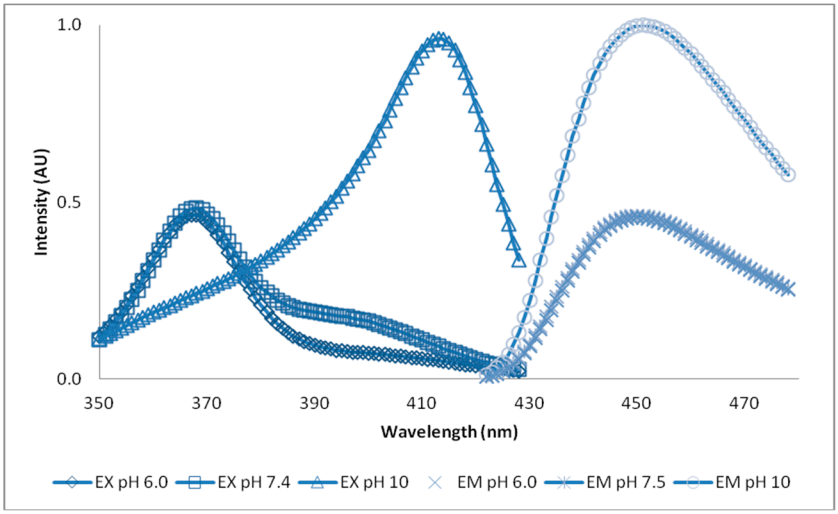

Figure 2. Spectral curves of excitation and emission for solutions of 7% gelatin with 0.9mM C3CA and 0.1mM 7HOC3CA.

3.2. C3CA Concentration

With sodium hydroxide with sodium bicarbonate solutions, varying the concentration of C3CA revealed a stronger response with concentrations 5 mM and greater, Figure 3. The peak normalized response, fluorescent intensity divided by dose, produced a decreasing exponential curve, Figure 4.

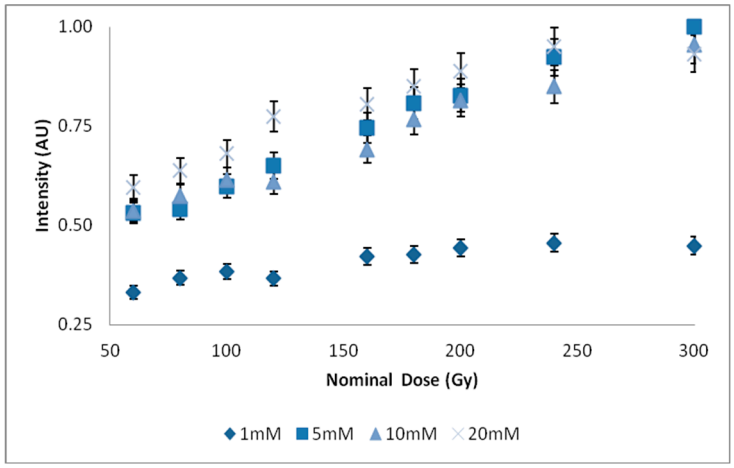

Figure 3. Nominal dose plotted against intensity for concentrations of C3CA in 7% gelatin. Error bars represent relative 5% error.

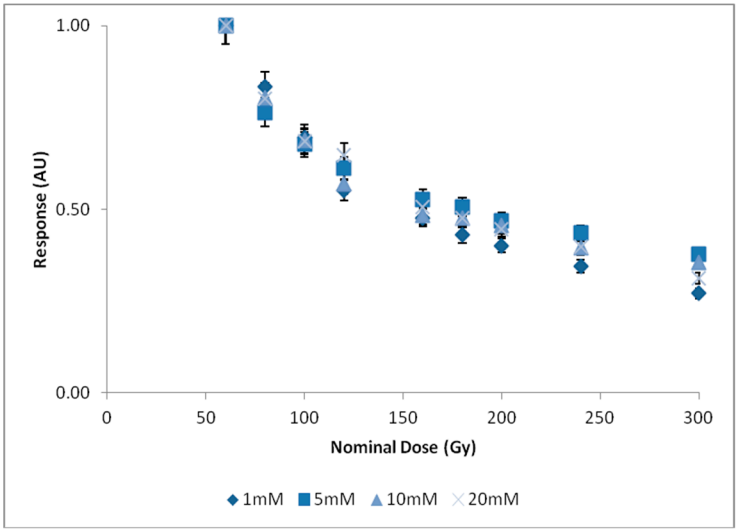

Figure 4. Nominal dose plotted versus normalized response. Error bars represent relative 5% error.

3.3. Dose Response

Dose response was studied with ionizing radiation with respect to type, rate, and energy. Relative response was measured with respect to 445nm emissions and plotted against nominal dose, Figure 5. Repeated measures, using four samples for each data point, demonstrated relative error less than 1%. A linear response was observed in the range investigated ($R > 0.99$), independent of type (photon or electron) and energy (9 MeV, 6 MV, and 23 MV), Figure 6. A strong negative correlation ($R > 0.99$) with dose rate was observed; the intensity of normalized fluorescent response decreased with increasing dose rate, Figure 7. Using a definition of three times the standard deviation of the background, the minimum detectable amount (MDA) was extrapolated from 9MeV electron data and estimated to be 1.5Gy, Figure 8.

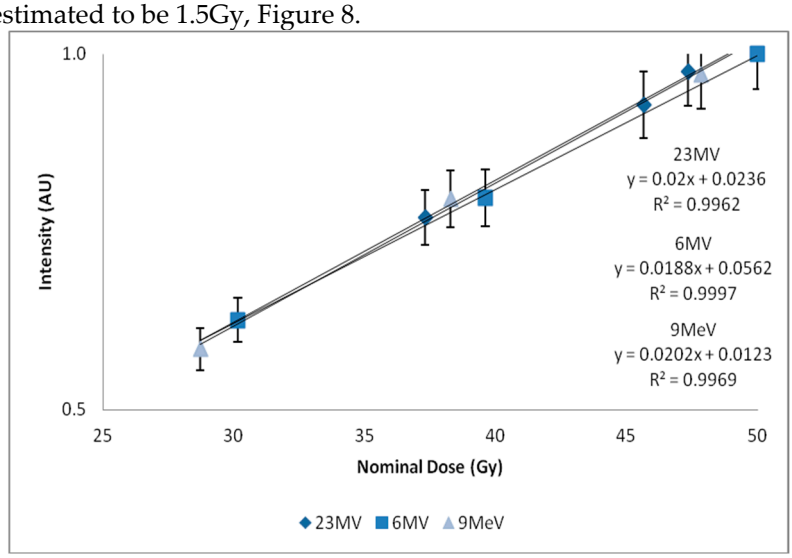

Figure 5. Nominal dose plotted against intensity, demonstrating a linear response (R>.99). Linear equations inlaid, error bars represent 5% relative error.

Preprints (www.preprints.org) | NOT PEER-REVIEWED | Posted: 11 May 2018 doi:10.20944/preprints201805.0176.v1

Peer-reviewed version available at Bioengineering 2018, 5, 53; doi:10.3390/bioengineering5030053

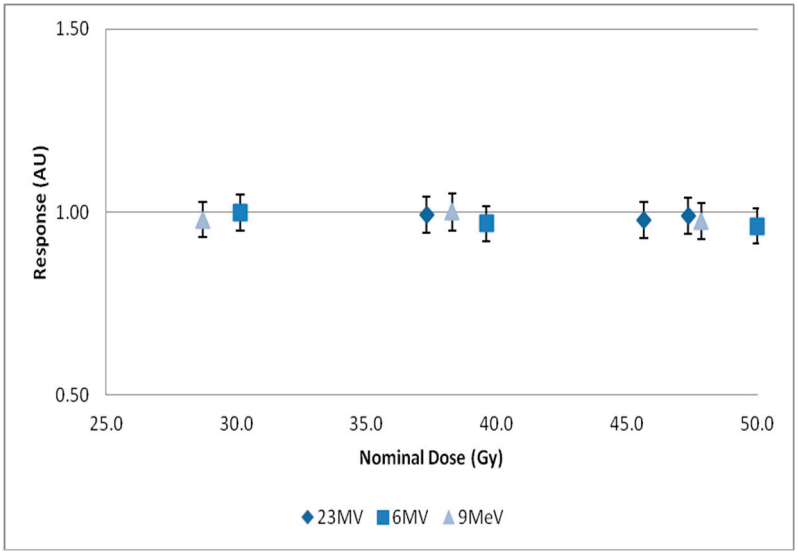

Figure 6. Normalized response plotted against nominal dose for 23 MV, 6 MV, and 9 MeV beams, error bars represent 5% relative error.

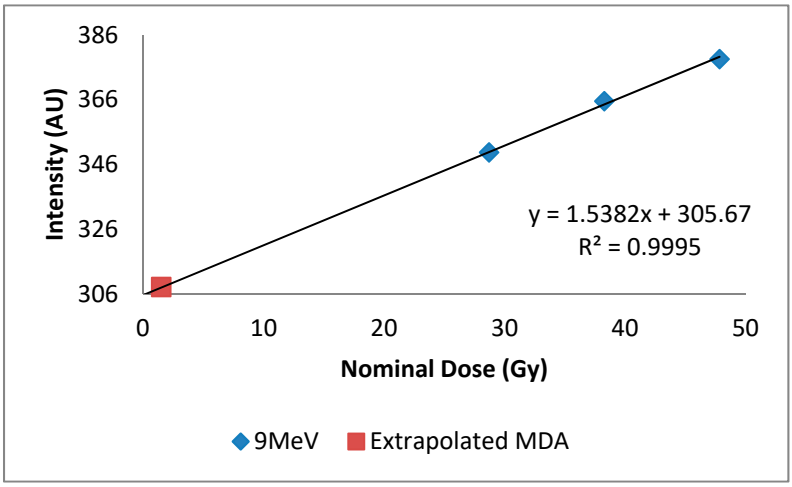

Figure 7. Plot of 9 MeV dose response plotted with extrapolated MDA.

4. Discussion

The basic solutions (pH 10) were observed to double emission intensity and shift the peak excitation wavelength from 365 nm to 405 nm. Transition between excited and ground states, the energy gap, is known to be influenced by the micro-environment through molecular motion, collision, rotational and translational diffusion, and formation of complexes. Smaller quantum yields are observed with large energy gaps due to availability of alternative relaxation pathways. The observed increase in quantum yield is consistent with previous studies in aqueous solution; however, greater than previously observed (385 nm) [22]. The increased spectral shift may be due to interactions with gelatin, additional study could clarify these effects.

The dose response was notably more pronounced for concentrations of C3CA above 5 mM. The normalized response curves of various concentrations of C3CA suggest saturation, diminishing population of radio-fluorogenic reactants in the dose range studied. Future work investigating absolute yields and a larger range of doses would be beneficial.

Normalized data demonstrate an independent linear response with respect to dose, energy, and type of ionizing radiation (electron and photon). With respect to type, an independent response is expected since photon dose deposition is predominately by delta rays, secondary electrons. A dose rate dependency was observed, consistent with other findings [20]. Previously suggested to be due

175 to metallic impurities in C3CA and alleviated by successive distillations. The MDA was estimated to
176 be 1.5 Gy, this value should be determined rigorously, by study of an expanded dose range.
177

178 **5. Conclusions**

179 Optical imaging of biomarkers is an active area of study with C3CA a recognized radiation
180 activated sensor for fluorescent imaging [18]. Investigators have explored the use of coumarin
181 attached to peptide ligands, designed for DNA binding, with potential for assessment of radiological
182 response [23]. Other work is currently studying the application of fluorescent labels for radiometric
183 assay [24, 25]. Advances in the fabrication of gelatin based phantom materials with 3D printability
184 make further study particularly attractive [26]. Further study radio-fluorescent sensors in a gelatin
185 matrix would help advance these prospective *in vivo* applications.
186 The potential of C3CA in gelatin for determination of spatial dose distributions has been
187 demonstrated in a separate report [27]. The use of planar laser induced fluorescence (PLIF) has been
188 shown as a method to yield high-resolution three-dimensional images [28]. This method of image
189 collection and analysis has been recognized and is currently being explored with polymer based
190 radio-fluorogenic gel [29]. However, it is the author's belief that the greatest depth of penetration
191 and finest imaging resolution will be obtained by applying methods of two-photon excitation
192 microscopy.

193 **Acknowledgments:** The first author would like to acknowledge the National Institute of Occupational Safety
194 for financial support during the performance of these studies. The first author would like to honor the memory
195 and impact of two of the co-authors who have passed prior to publication of this work. Howard Elson had a
196 wonderful tenure and a tremendous impact, not just on the first author, but an entire generation of medical
197 physicists trained at the University of Cincinnati. William Connick was a genuinely gifted professor whose time
198 on this earth was far too short; his intelligence, kindness, and authenticity will be remembered by many.

199 **Author Contributions:** P. Sandwall conceived and designed the experiments, B. Bastow supported the
200 performance the experiments; H. Spitz, H. Elson, M. Lamba, W. Connick, and H. Fenichel supported the
201 analysis of data and contributed reagents/materials/analysis tools. P. Sandwall wrote the paper.

202 **Conflicts of Interest:** The authors declare no conflict of interest.

References

1. Day, M. J., and Stein, G. Chemical effects of ionizing radiation in some gels. *Nature*, **1950**, 166(4212), 146.
2. Andrews, H. L., Murphy, R. E., and LeBrun, E. J. Gel dosimeter for depth-dose measurements. *Review of scientific instruments*, **1957**, *28*(5), 329-332.
3. Fricke, H., and Hart, E. J. The oxidation of the ferrocyanide, arsenite and selenite ions by the irradiation of their aqueous solutions with x-rays. *The Journal of Chemical Physics*, **1935**, *3*(9), 596-596.
4. Stein, G. and Tomkiewicz, M., Radiation chemistry of gelatin gels containing ferricyanide, radiation research, **1970**, 43(1), 25-33.
5. Gore, J. C., and Kang, Y. S. Measurement of radiation dose distributions by nuclear magnetic resonance (NMR) imaging. *Physics in Medicine & Biology*, **1984**, *29*(10), 1189.
6. Maryanski, M. J., Ibbott, G. S., Eastman, P., Schulz, R. J., and Gore, J. C. Radiation therapy dosimetry using magnetic resonance imaging of polymer gels. *Medical physics*, **1996**, *23*(5), 699-705.
7. Adamovics, J., and Maryanski, M. J. Characterisation of PRESAGE™: A new 3-D radiochromic solid polymer dosemeter for ionising radiation. *Radiation protection dosimetry*, **2006**, *120*(1-4), 107-112.
8. Warman, J. M., De Haas, M. P., and Luthjens, L. H. High-energy radiation monitoring based on radio-fluorogenic co-polymerization. I: small volume in situ probe. *Physics in Medicine & Biology*, **2009**, *54*(10), 3185.
9. Doran, S. J. The history and principles of chemical dosimetry for 3-D radiation fields: Gels, polymers and plastics. *Applied Radiation and Isotopes*, **2009**, *67*(3), 393-398.
10. Veis, A. *The Macromolecular Chemistry of Gelatin;* Academic Press, New York, NY, 1964.
11. Djagny, K.B., Wang, Z. and Xu, S. Gelatin: a valuable protein for food and pharmaceutical industries: Review, *Critical reviews in food science and nutrition*, **2001**, 41(6), 481-492.
12. Roussenova, M., Enrione, J., Diaz-Calderon, P., Taylor, A. J., Ubbink, J., and Alam, M. A. A nanostructural investigation of glassy gelatin oligomers: molecular organization and interactions with low molecular weight diluents. *New Journal of Physics*, **2012**, *14*(3), 035016.
13. Day, M.J. and Stein, G. Chemical Measurement of Ionizing Radiations, *Nature*, **1949**, 164(1), 671-672.
14. Stein, G. and Weiss, J. Detection of Free Hydroxyl Radicals by Hydroxylation of Aromatic Compounds, *Nature*, **1950**, 166(4235), 1104-1105.
15. Armstrong, W. A. and Grant, D. W. A highly sensitive chemical dosimeter for ionizing radiation. *Nature*, **1958**, 182(4637), 747-747.
16. Barreto, J. C., Smith, G. S., Strobel, N. H., McQuillin, P. A., and Miller, T. A. Terephthalic acid: a dosimeter for the detection of hydroxyl radicals in vitro. *Life sciences*, **1994**, *56*(4), PL89-PL96.
17. Matthews, R. W. Aqueous chemical dosimetry, *The International Journal of Applied Radiation and Isotopes*, **1982**, 33(11), 1159-1170.
18. Nadrowitz, R., Coray, A., Boehringer, T., Dunst, J., and Rades, D. (2012). A liquid fluorescence dosimeter for proton dosimetry. **2012**, *Physics in Medicine & Biology*, *57*(5), 1325.
19. Lakowicz, J. R. *Principles of Fluorescence Spectroscopy*, 3rd ed.; Springer, New York, NY, 2006
20. Collins, A.K., Makrigiorgos, G.M., and Svensson, G.K. Coumarin chemical dosimeter for radiation therapy. *Medical physics*, **1994**, 21(11), 1741-1747.
21. Yamashita, S., Baldacchino, G., Maeyama, T., Taguchi, M., Muroya, Y., Lin, M., Kimura, A., Murakami, T. and Katsumura, Y. Mechanism of radiation-induced reactions in aqueous solution of coumarin-3-carboxylic acid: effects of concentration, gas and additive on fluorescent product yield. *Free radical research*, **2012**, *46*(7), 861-871.
22. Dai, X., Rollin, E., Bellerive, A., Hargrove, C., Sinclair, D., Mifflin, C., & Zhang, F. Wavelength shifters for water Cherenkov detectors. *Nuclear Instruments and Methods in Physics Research Section A: Accelerators, Spectrometers, Detectors and Associated Equipment*, **2008**, *589*(2), 290-295.
23. Perry, C. C., Tang, V. J., Konigsfeld, K. M., Aguilera, J. A., and Milligan, J. R. Use of a coumarin-labeled hexa-arginine peptide as a fluorescent hydroxyl radical probe in a nanoparticulate plasmid DNA condensate. *The Journal of Physical Chemistry B*, **2011**, *115*(32), 9889-9897.
24. Gallina ME, Kim TJ, Vasquez J, Tuerkcan S, Abbyad P, and Pratx G. Single-cell analysis of radiotracers' uptake by fluorescence microscopy: direct and droplet approach. *Imaging, Manipulation, and Analysis of Biomolecules, Cells, and Tissues*, **2017,** 10068, 100680Y. International Society for Optics and Photonics.

25. Gallina ME, Kim TJ, Shelor M, Vasquez J, Mongersun A, Kim M, Tang SK, Abbyad P, and Pratx G. Toward a Droplet-Based Single-Cell Radiometric Assay. *Analytical chemistry* **2017**, 89(12):6472-81.
26. Dahal E, Badal A, Zidan A, Alayoubi A, Hagio T, Glick SJ, Badano A, and Ghammraoui B. Stable gelatin-based phantom materials with tunable x-ray attenuation properties and 3D printability for x-ray imaging. *Physics in medicine and biology*. **2018** Apr 10.
27. Sandwall, P. A., Spitz, H. B., Elson, H. R., Lamba, M. A., Connick, W. B., & Fenichel, H. Measuring the photon depth dose distribution produced by a medical linear accelerator in a water-equivalent radio-fluorogenic gel. *Journal of Radioanalytical and Nuclear Chemistry*, **2016**, *307*(3), 2505-2508.
28. Sandwall, P., Spitz, H., Elson, H., Lamba, M., Connick, W., & Fenichel, H. Radio-fluorogenic dosimetry with violet diode laser-induced fluorescence. In *Medical Imaging: Physics of Medical Imaging* **2014** (Vol. 9033, p. 90333Y). International Society for Optics and Photonics.
29. Yao T, Gasparini A, De Haas MP, Luthjens LH, Denkova AG, and Warman JM. A tomographic UV-sheet scanning technique for producing 3D fluorescence images of x-ray beams in a radio-fluorogenic gel. *Biomedical Physics & Engineering Express*. **2017**, 3(2):027004.